Blends of LDPE/Chitosan Using Epoxy-Functionalized LDPE as Compatibilizer

K. Prasanna,[1] R. R. N. Sailaja[2]

[1]*School of Mechanical and Building Sciences, VIT University, Vellore 632014, Tamilnadu, India*
[2]*The Energy and Resources Institute, EET (Energy Environment Technology) Division, Bangalore 560071, Karnataka, India*

Received 12 August 2010; accepted 8 June 2011
DOI 10.1002/app.35262
Published online 21 November 2011 in Wiley Online Library (wileyonlinelibrary.com).

ABSTRACT: LDPE and chitosan blends were prepared using an epoxy-functionalized polyethylene as compatibilizing agent for improving interfacial adhesion. Compatibilization improved both tensile and flexural properties (with values approaching close to that of neat LDPE) when compared with that of uncompatibilized blends. However, the elongation at break reduced due to the addition of rigid chitosan. Thermogravimetric analysis showed a two-stage degradation, while differential scanning calorimetry exhibited reduced crystallinity for compatibilized blends. Biodegradation studies revealed increased biodegradability with increase in chitosan loading. © 2011 Wiley Periodicals, Inc. J Appl Polym Sci 124: 3264–3275, 2012

Key words: LDPE; chitosan; compatibilizer; thermal and mechanical properties

INTRODUCTION

Plastics especially those used for packaging are used in large quantities, and their consumption is continuously on the rise. This leads to problems regarding plastic waste disposal owing to the nonbiodegradability of synthetic thermoplastics. Thus, owing to societal concerns and environment pollution, developmental efforts on various alternative solutions are being attempted. Among the various possible alternatives, biodegradable plastics are an eco-friendly and sustainable solution.

Microbial plastics based on polyhydroxyalkaonates are being used, but their cost is a major limitation. Another alternative is to blend the synthetic polymers like low-density polyethylene (LDPE) with biopolymers such as starch and cellulose.[1] However, a blend of LDPE with biopolymer will not be compatible because of their inherent differences in their chemical structure. Thus, to improve interfacial adhesion, compatibilizers are added to blend. Hence, this requires modification of either LDPE, biopolymer or both.[2–5]

Chitosan is the second most available abundant natural resource and is being used for a variety of applications. The unique features of biodegradability, biocompatibility, nontoxicity, and antibacterial characteristics of chitosan led to the development of a number of eco-friendly products. Hong et al.[6] coated polypropylene films with a number of polysaccharides such as methylcellulose, chitosan, and dextrin. It was inferred that coating based on chitosan and k-Caargeenan possess excellent mechanical properties and would act as antimicrobial agent carriers in active packaging systems. Chitosan and polyethylene oxide (PEO) films were found to have optimal mechanical properties at their stoichiometric composition as observed by Budtova et al.[7]

Similar observations by Osugi et al.[8] showed that a bilayered composite of chitosan–PEO blend possessed the best mechanical properties when compared with other variations. Chitosan test films were found to have antimicrobial properties with improved shelf life for food packaging as reported by Dutta et al.[9] The physical, mechanical, and antibacterial characteristics of chitosan/PEO films were examined by Zivanovic et al.[10] It was found that lower loading (10%) gave the optimal mechanical properties, while the water vapor permeability reduces with increase in chitosan fraction. Srinivasa et al.[11] studied the quality of mangoes kept in carton boxes in which the top surfaces were covered with chitosan films and another carton with an LDPE film. It was found that the former had an extended shelf life, whereas fungal growth and off-flavour was found for those covered with LDPE. Modified chitosan was added as a bioadditive for LDPE by Pasanphan et al.[12] Improved compatibility was observed between the two immiscible phases. A blend of LDPE with starch and chitin along with urea as plasticizer was prepared by Nino et al.[13] Ethylene-*co*-acrylic acid copolymer was used to

Correspondence to: R. R. N. Sailaja (rrnsb19@rediffmail.com).

enhance interfacial adhesion in the blend. The samples were found to undergo a weight loss in 30 days period.

Chitosan incorporated into an LDPE film was found to exhibit decreased tensile strength with increase in chitosan concentration, while elongation at break reduced drastically as observed by Park et al.[14] Similar observations were made by Zhang et al.[15] using different types of chitosan, including the water soluble derivative. Nisin and chitosan was incorporated in EVA copolymer by Lee et al.[16] It was suggested that the use of both nisin and chitosan was found to exhibit wide-spectrum antimicrobial characteristics. Active food packaging composed of a blend of LDPE with synthetic biodegradable polymers was studied by Nobile et al.[17] Similar observations were made on packaging of tomato and bell pepper using chitosan-based eco-friendly films.[18] To improve adhesion between linear low-density polyethylene (LLDPE) and chitosan or corn zein, the polyethylene was surface functionalized via plasma source implantation.[19] The commonly used polyethylenes are nonbiodegradable. Hence, to impart biodegradability, a biopolymer such as starch, cellulose, and chitosan has to be added. However, blends of nonpolar LDPE with a polar biopolymer are incompatible. Thus, to render the blend biodegradable, large loadings (>40%) are required. The blend thus prepared will have poor performance characteristics when compared with neat LDPE. Thus, to enhance their mechanical properties and at the same time include high loadings of the biopolymer, a compatibilizer consisting of both polar and nonpolar components would ensure proper dispersion of the biopolymer in the matrix. The well-dispersed blend will then have enhanced performance characteristics closer to that of neat LDPE when compared with an uncompatibilized blend.

Thus, in this study, biodegradable blends of chitosan with LDPE have been prepared. To improve the compatibility between LDPE and chitosan, an epoxy functionalized LDPE has been added as an interfacial modifier. The blend would then have the twin advantages of biodegradability and antibacterial characteristics, while the LDPE part would give strength and sealing capabilities to the packaging material. A small quantity ($\sim$ 0.1%) of prooxidant is also added to the blend to accelerate UV degradation of LDPE. The thermal, mechanical, and biodegradability characteristics of this blend have been investigated for varied loadings of chitosan and compatibilizer. No such studies could be cited in from literature.

MATERIALS AND METHODS

Materials

LDPE (grade 24FS040 with melt flow index 4 g/10 min.) was obtained from Saraswathi Plastics Bangalore, India. Chitosan (85% deacetylation) was obtained from Everest Biotech, Bangalore. Toluene, acetic acid, methanol, and common solvents were obtained from S.d Fine Chem, Mumbai. Poly (ethylene-*co*-glycidyl methacrylate) (PEGMA) obtained from Sigma–Aldrich (USA) was used as compatibilizer.

TABLE I
List of Blend Compositions

LDPE (g)	Chitosan (g)	PEGMA (g)
80	20.0	0.0
80	19.4	0.6
80	18.8	1.2
80	18.2	1.8
80	17.6	2.4
70	30.0	0.0
70	29.1	0.9
70	28.2	1.8
70	27.3	2.7
70	26.4	3.6
60	40.0	0.0
60	38.8	1.2
60	37.6	2.4
60	36.4	3.6
60	35.2	4.8
50	50.0	0.0
50	48.5	1.5
50	47.0	3.0
50	45.5	4.5
50	44.0	6.0
40	60.0	0.0
40	58.2	1.8
40	56.4	3.6
40	54.6	5.4
40	52.8	7.2

Preparation of blends

LDPE/chitosan weight ratios from 80–20 to 40–60 in 10% increment were prepared by varying the quantity of compatibilizer from 0 to 12 wt % of chitosan at 3% increment (Table I). The quantity of zinc sterate (Zn $(C_{18}H_{35}O_2)_2$) was kept constant at 0.1% of total weight. The preparation of the blend was carried out in the Brabender (Plasticorder, CMEI, 16CMESPL, East Germany). The blending time was carried out for 20 min at 130°C with a rotor speed of 20 rpm. The blends obtained from Brabender plasticorder were pressed into sheets in a compression mold (Hot Press Tester Labtech) at 15 MPa pressure and 120°C. The sheets were then cut into rectangular strips, and these strips were characterized for mechanical and thermal characteristics.

Mechanical properties of the blends

Tensile properties

The tensile properties of the blends and neat LDPE were measured by Zwick UTM (Zwick Roell, ZHU, 2.5) with Instron tensile flat surface grips at a cross

head speed of 2 mm/min. The tensile tests were performed as per ASTM D638 method. A minimum of five specimens were tested for each variation in composition of the blend and the obtained results were averaged.

Flexural properties

The flexural properties of the blends and pure LDPE were measured by Zwick UTM (Zwick Roell, ZHU, 2.5) with a preload speed of 10 mm/min. The tests were performed as per ASTM D 790-03 method. A minimum of five specimens were tested for each blend composition and the obtained results were averaged.

Thermal analysis of blends

Thermogravimetric analysis

Thermogravimetric analysis (TGA) was carried out for the blends and for pure LDPE using Perkin–Elmer Pyris Diamond 6000 analyzer [Perkin Elmer Inc, Shelten] in a Nitrogen atmosphere. The sample was subjected to a heating rate of 10°C/min in a heating range of 40–600°C with Al_2O_3 as reference material.

Differential scanning colorimetry

Differential Scanning colorimetry (DSC) of the blend specimen was carried out in a Mettler Toledo model DSC 822e instrument (Mettler Toledo AG, Switzerland). Samples were placed in sealed aluminum cells with a quantity of less than 10 mg and scanned at a heating rate of 10°C/min in a heating range of 50–150°C.

Blend morphology

Scanning electron microscopy (SEM) (JEOL, JSM–840) was used to study the morphology of the fractured and unfractured specimens. The specimens were gold sputtered (JEOL, SM-1100E) before microscopy. The SEM morphology of the unfractured specimens was determined after soaking the blend specimens for 24 h in 5% v/v sulphuric acid at room temperature.

Water absorption test

Water absorption of the blend specimens and the pure LDPE was carried out as per ASTM D570-81. The dried samples were weighed and submerged in distilled water at room temperature for 24 h. The excess water on the surface of the specimen after soaking is removed by wiping it with tissue paper, and the specimen was weighed again. The container without the soaking specimen is placed in an air oven at 50°C for 72 h to evaporate the water, and the water-soluble content obtained was equal to the increase of the dried container weight.

Biodegradation test

The Biodegradation of the blends specimen and the pure LDPE was carried out by soil burial method as per ASTM D5338-98. Soil-based compost was taken in small chambers. Humidity of the chambers was maintained at 40–45% by sprinkling water. The chamber were stored at 30–35°C. Rectangular-shaped specimens were buried completely into the wet soil at a depth of 10 cm. Samples were removed from the soil at constant time intervals (15 days) and washed gently with distilled water and dried in hot air oven at 50°C to constant weight. Weight loss percentages of the samples with respect to time were recorded as a measure of biodegradation.

RESULTS AND DISCUSSION

In this study, biodegradable blends of LDPE and chitosan have been prepared using glycidyl methacrylate grafted LDPE (PEGMA) as compatibilizer. The thermal, mechanical, morphological, water absorption. and biodegradability characteristics have been investigated for these blends.

FTIR spectroscopy

Figure 1 shows the FTIR spectroscopy of compatibilized blends containing 30 to 60% chitosan loading. The FTIR spectroscopy of pure chitosan is also shown in the figure for comparison. There are mainly four peaks for chitosan [curve (e)]. These include a broad peak at 3450 cm^{-1} due to inter and intramolecular hydrogen bonding between —OH and —CH_2OH groups. The peaks at 1633 cm^{-1} and 1567 cm^{-1} correspond to amide I and amide II bonds, while the peak at 1075 cm^{-1} is due to carbonyl (—C—O—) stretching. The blends of LDPE and

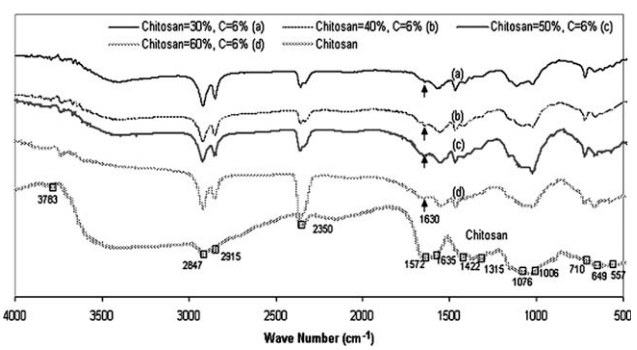

Figure 1 FTIR spectroscopy of compatibilized blends containing 30 to 60% chitosan loading and pure chitosan.

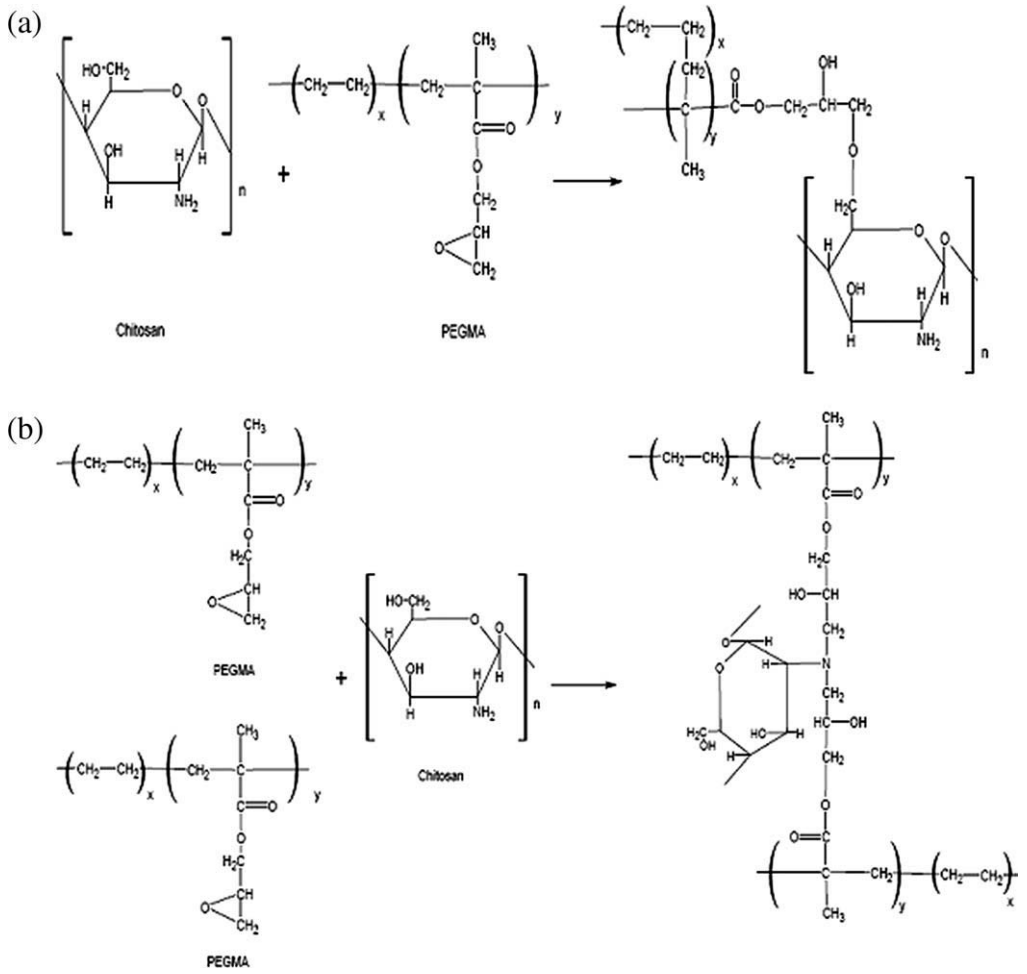

Figure 2 (a) and (b): Possible reaction scheme between Chitosan and compatibilizer (PEGMA) during reactive blending.

Chitosan has been prepared using epoxy-functionalized compatibilizer, i.e., PEGMA. The characteristic peak for the epoxy functional group occurs in the range of 899–925 cm^{-1}. The FTIR [curves (a–d)] spectrograms for the compatibilized blends do not show any peak in the above range indicating that the epoxy group has undergone scission by interacting with the hydroxyl and amide groups of chitosan during blending. The possible reaction schemes are shown in Figure 2(a,b). Curves (a) to (d) also include the characteristic peaks of LDPE, which includes peaks at 1460, 1014, and 715 cm^{-1} for $-CH_3$ asymmetric stretching, $-CH_2$ wagging, and $-CH_2$ rocking, respectively, while $-CH_2$ symmetric stretching peaks are at 2913 and 2844 cm^{-1} (shoulder peaks)

Engineering stress–strain curves

The engineering stress–strain curves are shown in Figure 3. All the blends (both uncompatibilized and compatibilized) exhibit brittle fracture although compatibilization shows a slight improvement in the strain values. As the chitosan loading increases, the stress values also increases although the strain values keep reducing owing to the inclusion of rigid Chitosan particles. The compatibilized blends for 20 and 60% chitosan loading show a significant improvement in stress values when compared with that of the uncompatibilized blends owing to better adhesion between the filler and LDPE which undergoes reactive blending by the scission of epoxy group in the compatibilizer as described earlier.

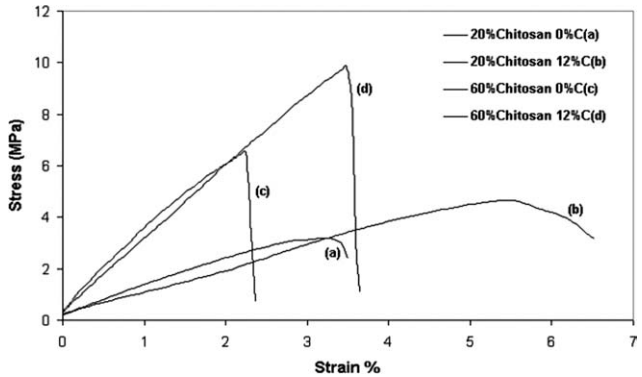

Figure 3 Stress/Strain curves for LDPE/chitosan blends.

For lower chitosan loading of 20%, the uncompatibilized blend [curve (a)] undergoes predominantly brittle failure, whereas it's compatibilized counterpart [curve (b)] exhibits improvement in stress and strain values. As chitosan loading increases to 60% [curve (c)], the uncompatibilized blends exhibit increased stress values but the specimens fail just after yielding. Compatibilization improves the interfacial interactions thereby increasing ductility and strength of the blend [curves (d) for the compatibilized counterpart of 60% chitosan loading)

Effect of compatibilizer

Figure 4 (a–c) shows the effect of compatibilizer in LDPE–chitosan blends. The relative tensile strength (RTS) versus percentage compatibilizer [Fig 4(a)] shows a decrease in strength as chitosan loading increases although compatibilization improves the interfacial adhesion. For, 20–40% of chitosan loading, compatibilized blends registered an increase in tensile strength values by more than 50% when compared with that of uncompatibilized blends, i.e., for 40% chitosan loadings, the RTS value is 1.13. This increase in RTS values for higher loadings of chitosan may be attributed to increased availability of reactive groups to react with the epoxy-functionalized compatibilizer.

The relative Young's modulus (RYM) versus percentage compatibilizer is plotted in Figure 4(b). The RYM values increases as the loading of rigid chitosan particles increases from 20 to 60%. Addition of compatibilizer helps anchoring the two immiscible phases together and thus improves stress transfer from the matrix to filler, thereby lowering the RYM values when compared with their uncompatibilized counterparts. The relative elongation at break (REB) reduces considerably as chitosan loading increases. Compatibilization slightly improves the REB values as observed in Figure 4(c) when compared with uncompatibilized blends.

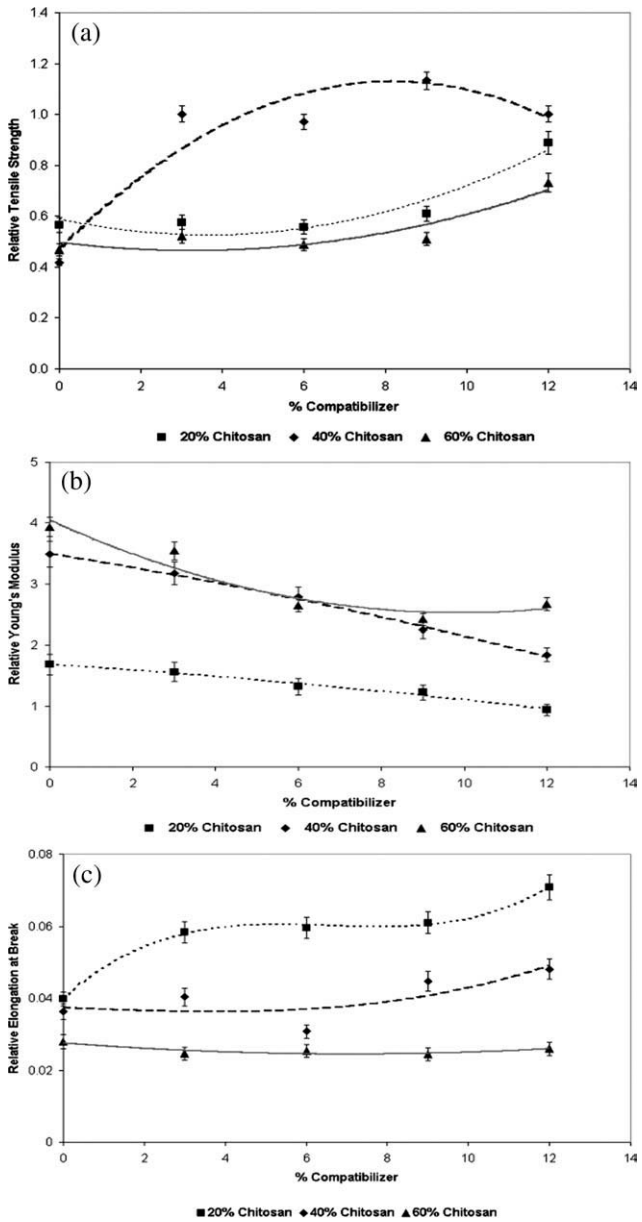

Figure 4 Plot of effect of compatibilizer on the mechanical properties for LDPE/chitosan blends. (a) Relative tensile strength versus percentage compatibilizer for the blends, (b) relative Young's modulus versus percentage compatibilizer for the blends, and (c) relative elongation at break versus percentage compatibilizer for the blends.

Relative tensile strength

Figure 5(a–c) shows the RTS values versus filler volume fraction (Φ) for LDPE–Chitosan blends for varying compatibilizer content. As chitosan loading increases, the RTS values also reduced as observed in Figure 5(a) for uncompatibilized blends. The RTS values keep increasing with compatibilizer addition as shown in Figure 5(b,c). The RTS value for 20% and 30% Chitosan loading reaches 0.89 and 0.88, respectively. For 40% and 50% loading, the RTS values reach the same value as that of neat LDPE. For still higher, i.e., 60% chitosan loading, the tensile strength value is 73% of that of neat LDPE. These high tensile strength values even with such high loadings of chitosan may be attributed to improved adhesion between LDPE and chitosan due to compatibilizer addition which undergoes reactive blending with chitosan.

Three theoretical models have been used to further analyze the obtained experimental results. The first is the Nicolais and Narkis model[20] is given below in eq. (1).

$$\mathrm{RTS} = \frac{\sigma_h}{\sigma_o} = 1 - 1.21\phi^{2/3} \quad (1)$$

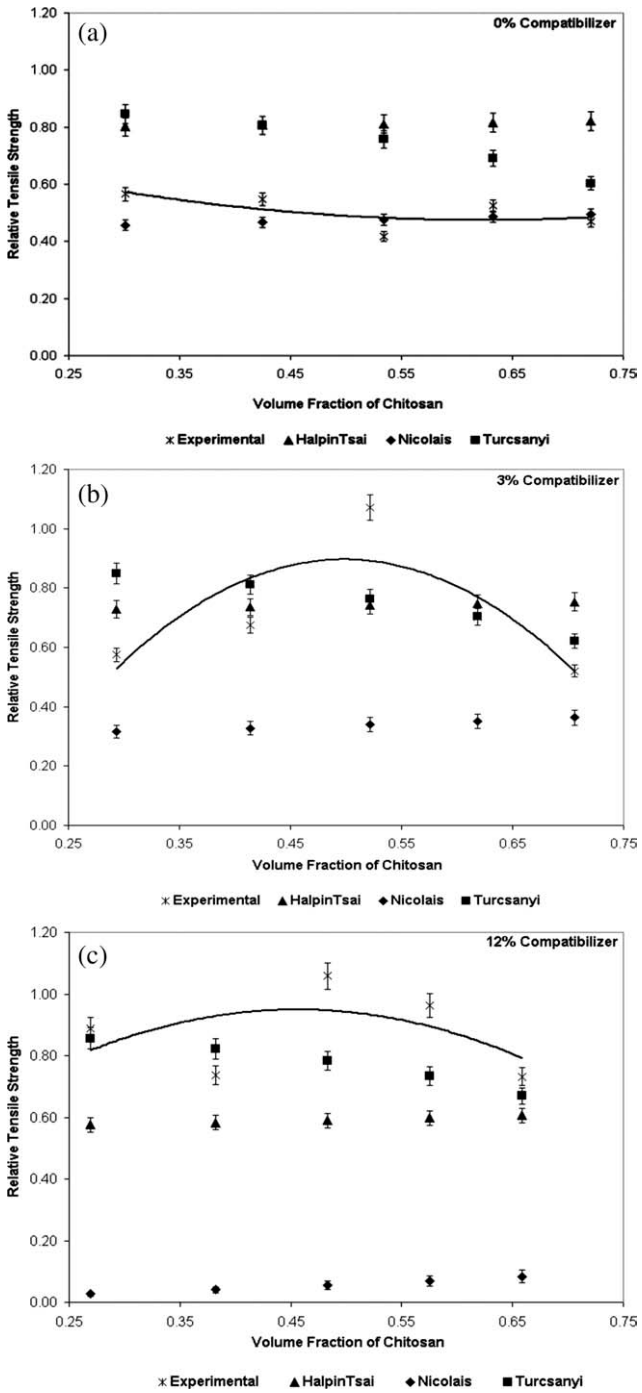

Figure 5 Variation of relative tensile strength with volume fraction of chitosan for (a) no compatibilizer; (b) 3% compatibilizer, and (c) 12% compatibilizer.

In eq. (1), σ_b and σ_O are the tensile strength values of the blend and neat LDPE, respectively, and ø is the volume fraction of chitosan. The volume fraction was calculated as follows,

$$\phi_i = \frac{(w_i/\rho_i)}{\sum(w_i/\rho_i)} \tag{2}$$

where, w_i and ρ_i are the density and weight fraction of component i, respectively. The density value of LDPE, PEGMA, and chitosan was taken to be 0.93, 0.94, and 0.54, respectively.[20,21]

The results obtained from eq. (1) are also plotted in Figure 5. The other model is the Halpin–Tsai model[20] for the tensile strength of the composite,

$$\text{RTS} = \frac{\sigma_b}{\sigma_o} = \frac{1 + G\eta_T\phi}{1 - \eta_T\phi} \tag{3}$$

where η_T is given by,

$$\eta_T = \frac{R_T - 1}{R_T + G} \text{ and } G = \frac{7 - 5\upsilon}{8 - 10\upsilon} \tag{4}$$

In the above eqs. (3) and (4), ν is the Poisson's ratio of LDPE taken to be as 0.43.[20] R_T values are found out by trial and error to match with the experimental results and this was found to be 0.45. The theoretical values obtained from eq. (3) are also plotted in Figure 5. The third model is a semiempirical model proposed by Turcsanyi for composition dependence on tensile strength and is as follows

$$\text{RTS} = \frac{\sigma_b}{\sigma_o} = \frac{1 - \phi}{1 + 2.5\phi}\exp(B\phi) \tag{5}$$

In eq. (5) above, B is a parameter dependent on interfacial adhesion. The value of B was found to be 2.5 as determined by trial and error to match with the experimental values. The theoretical values from eq. (5) are also plotted in Figure 5. From Figure 5(a), the experimental RTS values are closer to the Nicolais and Narkis when compared with other models for the uncompatibilized blends. This model assumes no adhesion between filler and matrix. This applies to uncompatibilized LDPE–Chitosan blends as the nonpolar hydrophobic LDPE does not interact with the polar hydrophilic Chitosan. Addition of epoxy-functionalized compatibilizer improves the adhesion between LDPE and Chitosan, and the theoretical values of the Halpin–Tsai model are a closer match to the obtained experimental values as observed in Figure 5(b,c). The Halpin–Tsai model assumes good adhesion between filler and matrix. The "B" value obtained for the Turcsanyi model is 2.5, which suggest good interfacial adhesion. Similar behavior has been observed for the blends of acrylonitrile–butadien–styrene (ABS) copolymer filled glass beads with a B value of 0.246, whereas the B value for the blend containing surface treated glass beads increased to 1.059 owing to increased interfacial adhesion.[21] The experimental results for uncompatibilized blends are matching with the results of Nicolais-Narkis model indicating poor interfacial adhesion. However, the observed RTS values for the compatibilized blends are closer to the theoretical values of Halpin-T-sai and Turcscanyi models.

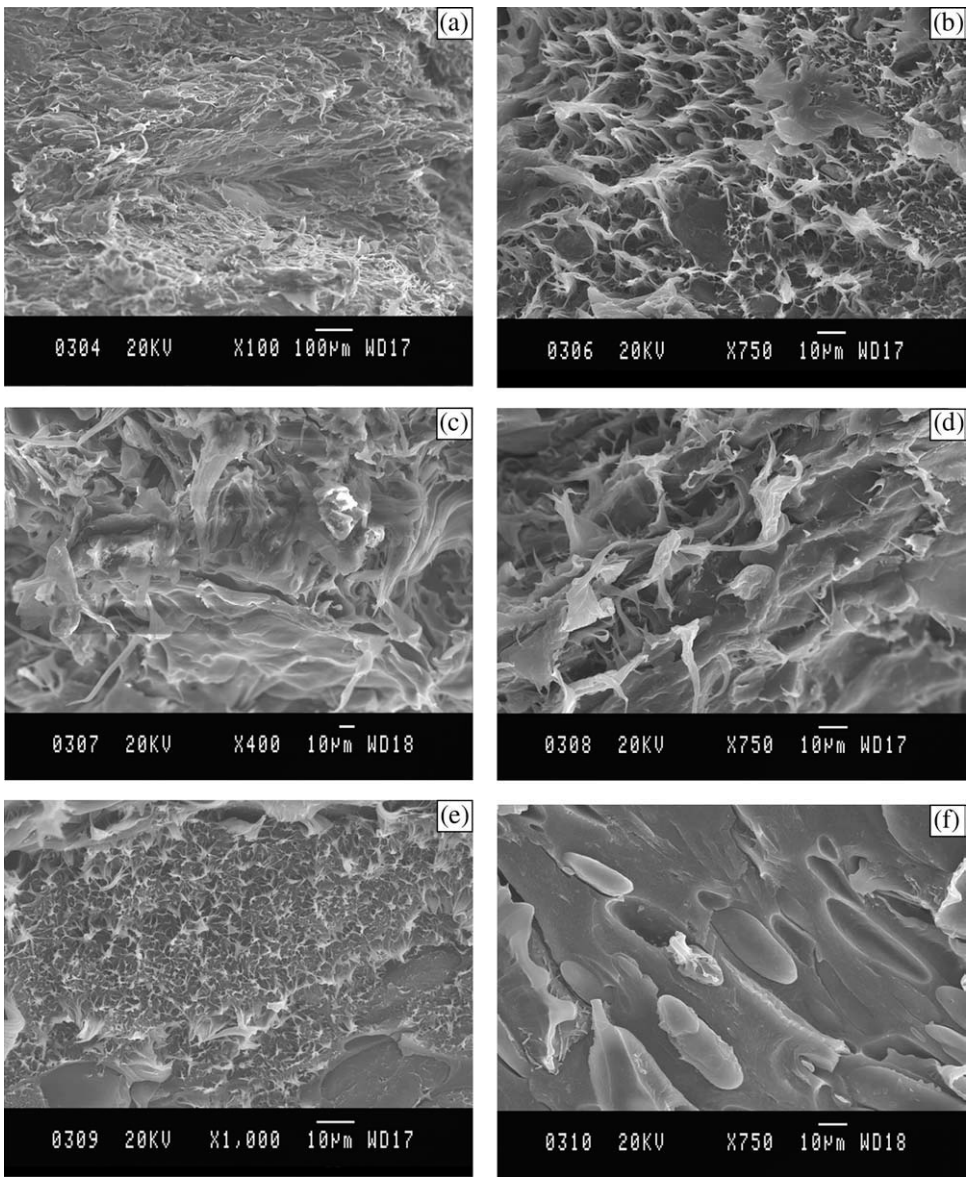

Figure 6 SEM photographs showing tensile fractured blend specimens (a) blend containing 20% chitosan and no compatibilizer, (b) blend containing 20% chitosan and 6% compatibilizer, (c) blend containing 40% chitosan and no compatibilizer, (d) blend containing 40% chitosan and 6% compatibilizer, (e) blend containing 60% chitosan and no compatibilizer, and (f) blend containing 60% Chitosan and 6% compatibilizer.

The RTS values for the compatibilized blends do not match with the theoretical results of the Nicolais and Narkis model.

The SEM morphology of the tensile fractured surfaces for LDPE–Chitosan blends is shown in Figure 6(a–f). The uncompatibilized blend with 20% chitosan exhibits quasi-brittle fracture [Fig. 6 (a)] indicating that the matrix is able to withstand low loadings. The compatibilized counterpart [Fig. 6(b)] shows a uniform dimpled network with sheared short fibril bundles along with debonded chitosan particles indicating uniform dispersion leading to partially ductile failure. This is also reflected in high RTS values close to that of neat LDPE (89% of pure LDPE). For higher loading of 40% [Fig. 6(c)] loading, quasi brittle fracture characterized by sheared matrix and large holes left by agglomerated and debonded chitosan particles. The compatibilized blend [Fig. 6(d)] also exhibits a quasi brittle fracture with thinner bundles of sheared matrix spread over the entire fracture surface. Compatibilization leads to better dispersion of chitosan due to improved adhesion with the matrix leading to better stress transfer from the matrix to the filler and thus improves the RTS value to 1.06. For 60% chitosan loading, blend exhibits a typical brittle fracture surface (uncompatibilized blend shown in [Fig. 6(e)] characterized by short fibrils giving the appearance of dimpled network. The compatibilized blend shown in [Fig. 6(f)] shows that phase inversion has taken place. The debonded

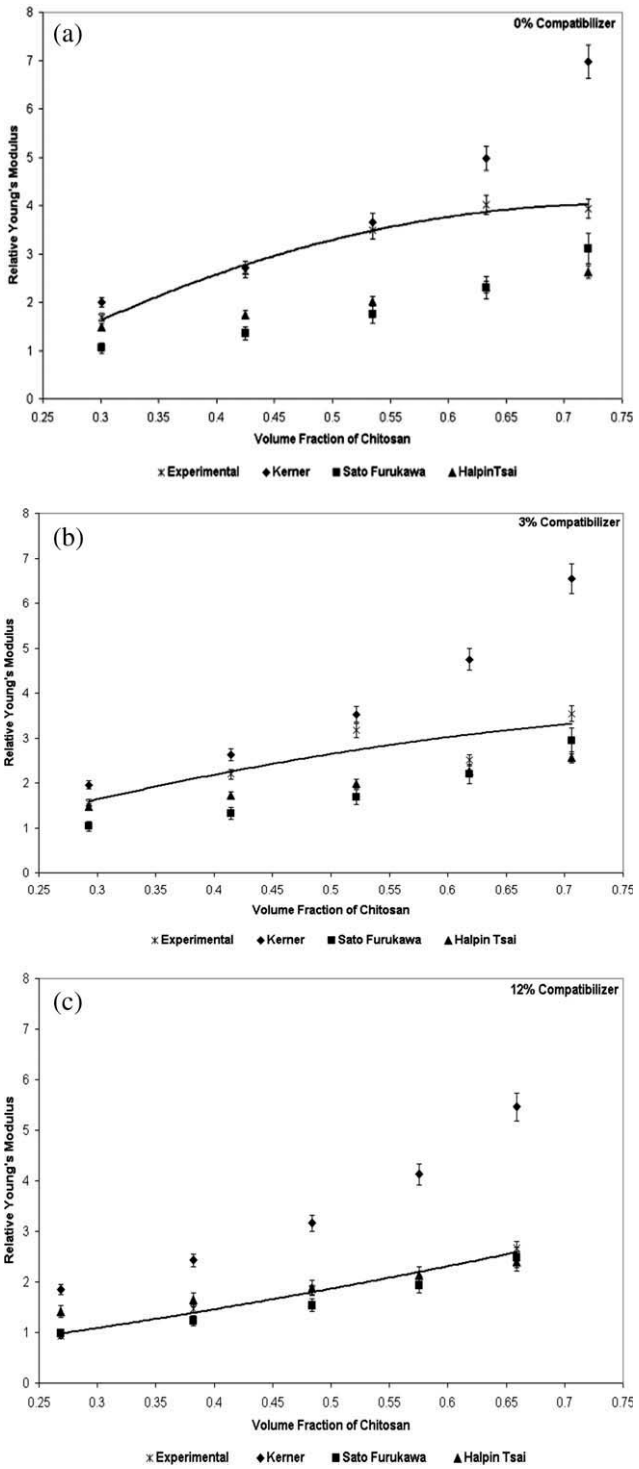

Figure 7 Plot of relative Young's modulus with volume fraction of chitosan for (a) no compatibilizer, (b) 3% compatibilizer, and (c) 12% compatibilizer.

LDPE particles have undergone crazing before debonding from the chitosan matrix.

Relative Young's modulus

The RYM versus filler volume fraction for various compatibilizer contents is shown in [Fig. 7(a–c)]. The RYM values increase with increase in filler loading due to the stiffness of rigid chitosan particles [Fig. 7(a)]. For the compatibilized blends, the RYM values reduce and the values are closer to neat LDPE owing to better interaction between LDPE and chitosan due to reaction between PEGMA and chitosan.

Three theoretical models have been examined to further analyze the obtained experimental results. The first is the Kerner's model,[20] which assumes no adhesion between filler and matrix and is given below in eq. (6).

$$\mathrm{RYM} = \frac{E_b}{E_{\mathrm{LDPE}}} = 1 + \left(\frac{\phi}{1-\phi}\right)\left(\frac{15(1-\upsilon)}{(8-10\upsilon)}\right) \tag{6}$$

In eq. (6), E_b and E_{LDPE} is the Young's modulus of the blend and neat LDPE, respectively. The theoretical values obtained using eq. (6) are also plotted in Figure 7. The second model is the Halpin–Tsai model[20] given below in eq. (7),

$$\mathrm{RYM} = \frac{E_b}{E_{\mathrm{LDPE}}} = \frac{1 + G\eta_m\phi}{1 - \eta_m\phi} \tag{7}$$

where,

$$\eta_m = \frac{R_m - 1}{R_m + G} \tag{8}$$

In eq. (8), R_m is the ratio of filler tensile modulus to matrix tensile modulus. An R_m values were found by trial and error to match with the experimental results and thus was found to be 4.1. The theoretical values thus determined are plotted in Figure 7.

The third model is the Sato-Furukawa model[21] for estimating the extent of interfacial adhesion is given in eq. (9) below,

$$\mathrm{RYM} = \frac{E_b}{E_{\mathrm{LDPE}}} = \left[\left(1 - \frac{\phi^{2/3}}{2 - 2\phi^{1/3}}\right)(1 - \psi\xi) - \frac{\phi^{2/3}\psi\zeta}{(1-\phi^{1/3})\phi}\right] \tag{9}$$

where, Ψ is given by,

$$\psi = \left(\frac{1 + \phi^{1/3} - \phi^{2/3}}{1 - \phi^{1/3} + \phi^{2/3}}\right) \tag{10}$$

In eq. (9), above ξ is the adhesion parameter which varies from 0 to 1 for perfect adhesion to no adhesion, respectively. The ξ value found by trial and error was determined to match with the experimental results and was found to be 0.7, which indicates that the interfacial adhesion is between the two extremes. The results obtained from eq. (9) are also

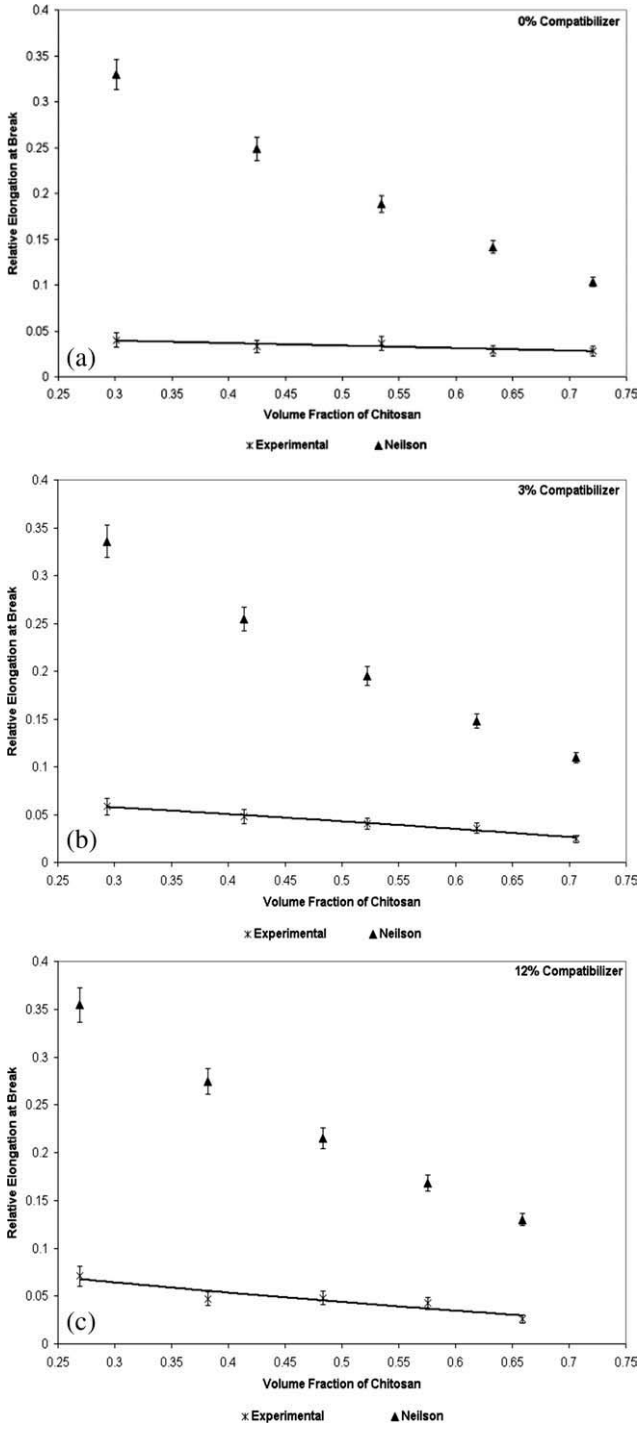

Figure 8 Plot of relative elongation at break with volume fraction of chitosan for (a) no compatibilizer; (b) 3% compatibilizer, and (c) 12% compatibilizer.

plotted in Figure 7. The experimental results for the uncompatibilized blends [Fig. 7(a)] are closer to the values obtained by Kerner's model suggesting a lack of adhesion. For the compatibilized blends [Fig. 7(b,c)], the obtained results are closer to those obtained by Halpin—Tsai and Sato-Furukawa model indicating that the epoxy-functionalized compatibilizer could effectively anchor with the two immiscible phases.

Relative elongation at break

Figure 8(a–c) shows the REB values versus filler volume fraction. The REB values reduce drastically as the rigid chitosan particles do not undergo elongation and thus, reduce the effective load bearing area.

Compatibilization marginally improves the REB values but they are much lesser than neat LDPE. For immiscible blends, there is a trade off between increase of tensile strength and elongation values by adding a compatibilizer. Nielsen's model for perfect adhesion is given below in eq. (11) for analyzing the obtained REB values as follows[20]

$$\mathrm{REB} = \frac{\epsilon_b}{\epsilon_{\mathrm{LDPE}}} = \left(1 - 1.21\phi^{2/3}\right) \tag{11}$$

where, ϵ_b and ϵ_{LDPE} is the elongation at break for the blend and neat LDPE, respectively. The experimental values do not match with the obtained experimental results as perfect adhesion is not possible for immiscible blends.

Flexural strength

Figure 9 shows the effect of compatibilizer on the relative flexural strength (RFS) of LDPE–Chitosan blends. The flexural strength increases with increasing chitosan loading for uncompatibilized blends. This may be attributed to higher tensile strength of chitosan. However, compatibilized blends showed enhanced RFS values as observed in Figure 9. For 20% of chitosan loading, the RFS values increase from 0.27 to value close to that of neat LDPE with a RFS value of 0.96. For 30% of chitosan loading, the

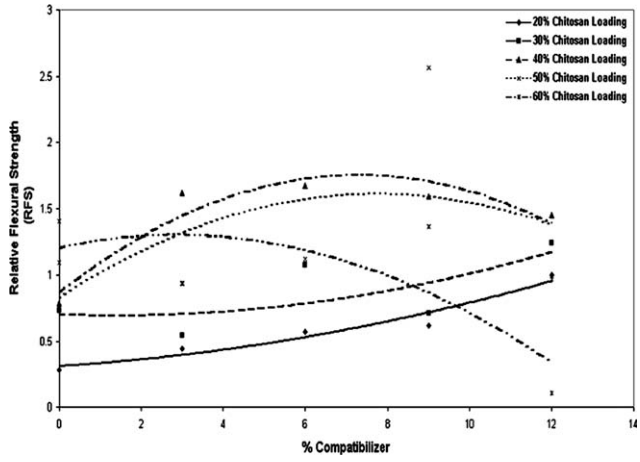

Figure 9 Plot of effect of compatibilizer on the relative flexural strength of LDPE/chitosan blends.

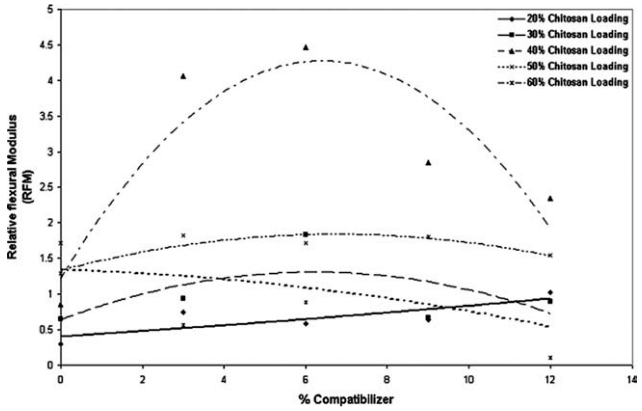

Figure 10 Plot of effect of compatibilizer on the relative flexural modulus of LDPE/chitosan blends.

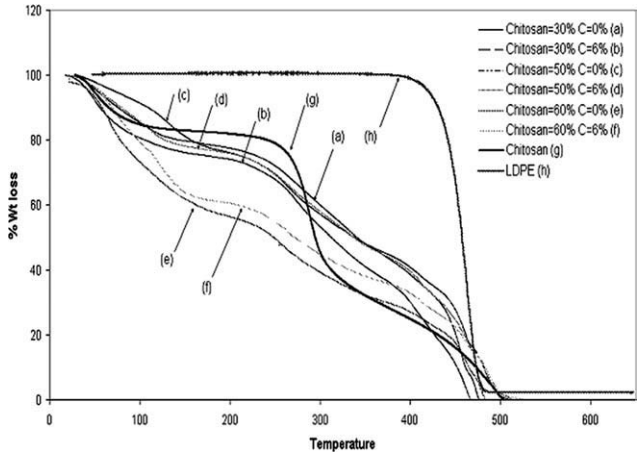

Figure 11 TGA thermograms for LDPE/chitosan blends.

maximum RFS value is 1.33, i.e., 33% higher than neat LDPE. For higher loadings of 40 and 50%, the optimal RFS values are 1.67 and 1.73, respectively. The increase in flexural strength is attributed to the stiffness of chitosan and better stress transfer from LDPE to chitosan owing to the reactive blending with the epoxy-functionalized compatibilizer. For all compositions, there exists an optimum compatibilizer content (6%) beyond which the RFS values reduce due to the presence of excessive compatibilizer which tends to form a third phase.

Flexural modulus

The relative flexural modulus (RFM) for LDPE/Chitosan blends is shown in Figure 10. The RFM values increase on increasing chitosan loading from 20 to 60% owing to the stiffness of chitosan chains. Compatibilization further enhances these values in each case and an optimal compatibilizer content of 6% is observed similar to the trend for RFS values. For 20 and 30% of chitosan loading, the maximum RFM values are 0.75 and 1.82, respectively. For 40–60%, the RFM values are close to 3.5 indicating better stress transfer leading to efficient reactive compatibilization.

Thermogravimetric Analysis

Figure 11(a) shows the TGA curves of LDPE/Chitosan blends. The TGA curves of neat LDPE and chitosan are also given in the figure for comparison. Neat LDPE and Chitosan show a single-stage degradation. The onset of degradation for neat LDPE is at 398°C, whereas that of pure chitosan is at 254°C. The degradation peaks for LDPE and Chitosan are, respectively, at 464.6°C and 290°C. The degradation of neat LDPE is characterized by the breakage of —C—C— backbone, whereas the degradation of chitosan is complex, which is characterized by the release of pyrolysis products such as CO, CO_2, and other volatiles between 207 and 319°C.[22] The degradation of chitosan involves dehydration, deacetylation, and chain scission.[23]

The DTG for the blends containing 30, 50, and 60% chitosan loading are also shown in Figure 11(b). For 30% and 50% of chitosan loadings, the uncompatibilized blends mainly exhibit a two-stage degradation. The peak below 120°C is mainly attributed to the loss of absorbed water from the materials. The first degradation peak is at 243°C (broad) with 27% weight loss for 30% chitosan-loaded blends, whereas for 50% chitosan loadings, this peak is at 267°C with 35% weight loss. The second degradation peak with maximum weight loss is 456°C (85% weight loss) and 483°C (91% weight loss) for 30% and 50% chitosan loading.

The compatibilized counterparts for 30% and 50% chitosan loading exhibit degradation peaks at slightly lower temperatures. The peaks temperatures for 30% and 50% chitosan loading are at 274°C (with 40% weight loss) and at 265°C (with 36% weight loss), respectively, mainly characterized by broad peaks. The corresponding peak for 60% chitosan

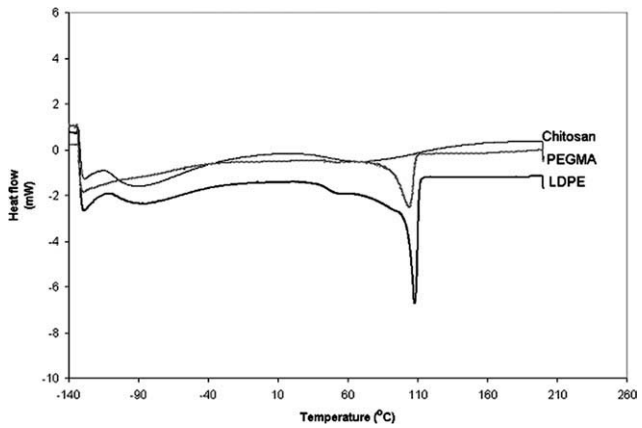

Figure 12 DSC thermograms for LDPE/chitosan blends.

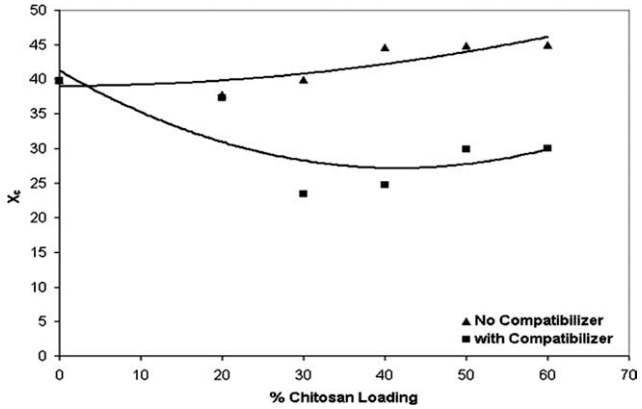

Figure 13 Plot of change in X_c values for LDPE/chitosan blends.

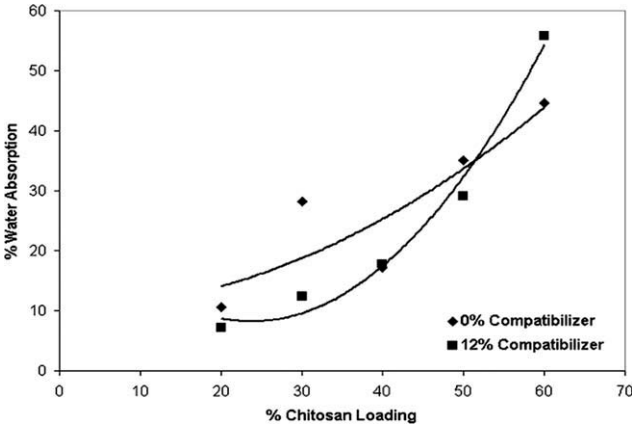

Figure 14 Plot of water absorbency for uncompatibilized and compatibilized LDPE/chitosan blends.

loading occurs at 262°C (with 48% weight loss) due to degradation of chitosan. The second degradation peak for 30%, 50%, and 60% chitosan loading are, respectively, at 422°C (with 79% weight loss), 484°C (93% weight loss), and 482°C (89% weight loss). The char formations for the uncompatibilized blends are higher than for the compatibilized counterparts because of increased interactions between the blend components.

DSC thermograms

The DSC thermograms for LDPE, chitosan, and PEGMA are shown in Figure 12. The melting peak for neat LDPE is observed at 108°C. The epoxy grafted compatibilizer exhibits a melting peak at 105°C. The DSC thermograms for LDPE–chitosan blends are shown in Figure 13. For uncompatibilized blends with 30% and 40% chitosan loading, the thermogram exhibits a single peak at 109°C accompanied a shoulder peak at 86.5°C. The compatibilized counterpart shows two peaks characterized by a small broad peak at −3.5°C and another peak at 109°C. For 60% chitosan loading, too, the trend is similar.

The percentage crystallinity (X_c) of the LDPE phase in the blends is determined using the equation given below

$$X_c = \frac{\Delta H_f}{\Delta H_f^o} \times 100 \qquad (12)$$

In eq. (12) above, ΔH_f is the heat of fusion for the blends. ΔH^o_f is the heat of fusion for 100% crystalline LDPE, taken to be 287.63 J/g.[24] Figure 13 shows the change in X_c values for LDPE/chitosan blends. The X_c values for uncompatibilized blends are slightly higher than of neat LDPE due to the addition of chitosan. Similarly, observations have been made for certain other polyolefin blends.[25–27] It was suggested that this occurs due to nucleation and positive deviations from the rule of additivity. The compatibilized blends, however, exhibit reduced X_c values when compared with neat LDPE owing to increased interactions between the blend components. The grafted long GMA units of the compatibilizer exist in the amorphous region. These long noncrystallizable grafted chains interrupt or terminate nucleation along the polymer chains. A similar observation has been made for GMA grafted polystyrene blends by Gao et al.[28]

Water absorbency

Figure 14 shows the water absorbency for uncompatibilized and compatibilized LDPE–chitosan blends for chitosan loading varying from 20 to 60%. The absorption (AB) of the blends is calculated by the eq. (13) given below:

$$\mathrm{AB} = (W_1 - W_o + W_{sol})/W_o \qquad (13)$$

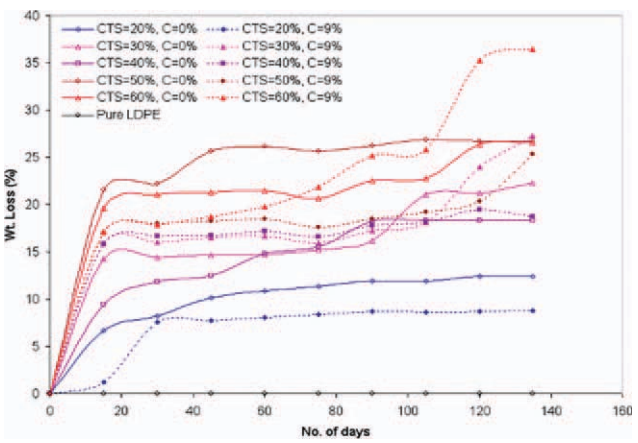

Figure 15 Plot of percentage weight loss of LDPE/chitosan blends versus number of days. [Color figure can be viewed in the online issue, which is available at wileyonlinelibrary.com.]

where W_1, W_o, and W_{sol} are the weight of the specimen containing water, the weight of the dried specimen, and the weight of the water-soluble residuals, respectively. The water absorbency increases with increase in chitosan loading. The uncompatibilized blends exhibit higher water absorption than compatibilized blends upto 50% chitosan loading. Compatibilization improves dispersion of chitosan in LDPE matrix. Thus, the chitosan particles are enveloped in LDPE, thereby improving the water resistance. However, for higher, i.e., 60% Chitosan loading, the compatibilized blend exhibits higher water absorbency than its uncompatibilized counterpart as in this case, chitosan is the predominant component in the blend.

Biodegradation

Figure 15 shows a plot of percentage weight loss of LDPE/chitosan blends versus number of days. The curve for the LDPE/chitosan blends decrease in weight upto 135 days, whereas LDPE shows insignificant change in weight within the same period. As chitosan loading is increased, degradation rate of the blends also increased. These results indicate that the chitosan molecules act as a nutrient source for microbial growth resulting in the initiation of degradation of LDPE/chitosan blends. Similar results were obtained in a computer simulation study of the degradation of starch/polyethylene blends.[29] Maximum weight loss of 36% is obtained for blends with 60% chitosan loading and 9% compatibilizer. The trend in degradation rate is similar for both compatibilized and uncompatibilized blends. The prooxidant also facilitates the UV degradation of the matrix.

CONCLUSIONS

LDPE/chitosan blends were studied using PEGMA as compatibilizer. The mechanical properties were found to improve considerably even for high loadings due to the addition of a compatibilizing agent. The epoxy group of the compatibilizer undergoes scission and thus undergoes reactive blending with the hydroxyl and amide groups of chitosan. Because of enhanced interaction between LDPE and chitosan, better stress transfer from matrix to filler leads to considerable improvements in the mechanical properties especially tensile strength and flexural strength, although the elongation at break values reduced. The thermogravimetric analysis revealed that LDPE/chitosan blends exhibits a two-stage degradation. The DSC analysis showed a reduced crystallinity for the compatibilized blends owing to increased interactions between the blend components. Biodegradation and water absorption characteristics increased with increase in chitosan loading.

References

1. Sailaja, R. R. N.; Chanda, M. J Appl Polym Sci 2001, 80, 863.
2. Sailaja, R. R. N.; Reddy, A. P.; Chanda, M. Polym Int 2001, 50, 1352.
3. Sailaja, R. R. N. Polym Int 2005, 54, 1589.
4. Girija, B. G.; Sailaja, R. R. N. J Appl Polym Sci 2006, 101, 1109.
5. Sailaja, R. R. N.; Seetharamu, S. J Appl Polym Sci 2009, 112, 649.
6. Hong, S.; Lee, J.; Son, S. Packaging Technol Sci 2005, 18, 1.
7. Budtova, T.; Belnikevich, N.; Kalyuzhnaya, L.; Alexeev, V.; Bronnikov, S.; Vesnebolotskaya, S.; Zoolshoev, Z. J Appl Polym Sci 2002, 84, 1114.
8. Osugi, N.; Dong, T.; Hexig, B.; Inoue, Y. J Appl Polym Sci 2007, 104, 2939.
9. Dutta, P. K.; Tripathi, S.; Mehrotra, G. K.; Dutta, J. Food Chem 2009, 114, 1173.
10. Zivanovic, S.; Li, J.; Davidson, P. M.; Kit, K. Biomacromolecules 2007, 8, 1505.
11. Srinivasa, P. C.; Baskaran, R.; Ramesh, M. N.; Prashanth, K. V. H.; Tharanathan, R. N. J Eur Food Res Technol 2002, 215, 504.
12. Pasanphan, W.; Buettner, G. R.; Chirachanchai, S. J Appl Polym Sci 2008, 109, 38.
13. Nino, K. A.; Imam, S. H.; Gordon, S. H.; Wong, L. J. B. ACS symp Ser 1999, 723, 198.
14. Park, S. I.; Marsh, K. S.; Dawson, P. L.; Acton, J. C.; Han, I. Institute of Food Technologists Annual Meeting, Anaheim, California, USA, June 19, 2002.
15. Zhang, H.; Gu, C. H.; Wu, H.; Fan, L.; Li, F.; Yang, F.; Yang, Q. BioFactors 2008, 30, 227.
16. Lee, C. H.; An, D. S.; Park, H. J.; Lee, D. S. Packaging Technol Sci 2003, 16, 99.
17. Nobile, M. A. D.; Conte, A.; Buonocore, G. G.; Incoronato, A. L.; Massaro, A.; Panza, O. J Food Eng 2009, 93, 1.
18. Srinivasa, P. C.; Prashanth, K. V. H.; Susheelamma, N. S.; Ravi, R.; Tharanathan, R. N. J food Sci Agri 2006, 86, 1216.
19. Shin, G. H.; Lee, Y. H.; Lee, J. S.; Kim, Y. S.; Choi, W. S.; Park, H. J. J Agric Food Chem 2002, 50, 4608.
20. Willett, J. L. J Appl Polym Sci 1994, 54, 1685.
21. Bliznakov, E. D.; White, C. C.; Shaw, M. T. J Appl Polym Sci 2000, 77, 3220.
22. Faria, E. A.; Prado, A. G. S. Reac Func Polym 2007, 67, 655.
23. Don, T.; Chuang, C.; Chiu, W. Tam-kang J Sci Engg 2002, 5, 235.
24. Hatakeyama, T.; Liu, Z. Handbook of Thermal Analysis; John Wiley: England, 1998.
25. Minkova, L.; Yordanov, H.; Zamfirova, G.; Magagnini, P. L. Colloid Polym Sci 2002, 280, 358.
26. Rath, T.; Kumar, S.; Mahaling, R. N.; Mukherjee, M.; Das, C. K.; Pandey, K. N.; Saxena, A. K. Polym Compos 2006, 27, 533.
27. Privalko, E. G.; Pedosenko, A. V.; Privalko, V. P.; Walter, R.; Friedrich, K. J Appl Polym Sci 1999, 73, 1267.
28. Gao, Y.; Li, H.; Wang, X. Eur Polym J 2007, 43, 1258.
29. Peanasky, J. S.; Long, J. M.; Wool, R. P. J Polym Sci Polym Phys 1990, 29, 565.